의학박사 학위논문

폐암 조직의 마이크로바이옴과 병리학적 및 임상적 매개변수와의 연관성

The microbiome of lung cancer tissue and its association with pathological and clinical parameters

울 산 대 학 교 대 학 원

의 학 과

김 옥 화

The microbiome of lung cancer tissue and its association with pathological and clinical parameters

지 도 교 수　이 세 원

이 논문을 의학박사 학위 논문으로 제출함

2021 년 8 월

울 산 대 학 교　대 학 원

의　학　과

김 옥 화

김옥화의 의학박사학위 논문을 인준함

심사위원 김 동 관

심사위원 이 재 철

심사위원 노 진 경

심사위원 설 우 준

심사위원 이 세 원

울 산 대 학 교 대 학 원

2021 년 8 월

감사의 글

많이 부족한 저이지만 여러 분들의 도움의 손길로 무사히 박사 과정을 마무리할 수 있었습니다. 도움을 주신 많은 분들께 이 글을 통해 감사의 인사를 드리고자 합니다.

먼저 이 연구의 방향을 제시해 주시고, 아낌없는 지도를 해 주신 이세원 교수님께 감사드립니다. 교수님께서는 학문에 대한 끝없는 열정으로 참된 연구자의 자세를 보여주셨을 뿐만 아니라 전 박사 과정동안 큰 도움을 주셨고, 논문이 마무리될 때까지 세심한 조언을 아끼지 않으셨습니다. 이 글을 통해 다시 한번 진심으로 감사드립니다.

또한 실험 과정 및 결과 분석에 많은 도움을 주신 최보윤 선생님, 설우준 교수님께 감사드립니다. 그리고 바쁘신 와중에도 논문 심사를 위해서 귀중한 시간을 내주시고 논문의 내용과 연구 전반에 대하여 조언을 해 주신 김동관 교수님, 이재철 교수님, 노진경 교수님, 설우준 교수님께 다시 한번 감사드립니다. 훌륭하신 교수님들을 본받아 항상 최선을 다하는 모습을 보여드리도록 노력하겠습니다.

독박 육아를 마다하지 않고 전폭적인 지지와 내조를 보여준, 세상에서 가장 사랑하는 저의 반려자 임익주에게 언제나 저를 믿어주고 격려해주며 채찍질해 준 것에 대해 감사하며 사랑한다고 전합니다. 그리고 새로운 가족이 되어 무한한 행복과 기쁨을 선사하는 사랑하는 아들 도윤이에게도 사랑을 듬뿍 담아 감사의 인사를 전합니다. 하늘 나라에서 항상 저를 지켜봐 주시고 제가 바른 길을 가도록 인도해주시는 아버지, 생각만으로도 늘 편안한 마음의 쉼터가 되어 주시는 어머니, 언제나 든든한 지원군, 버팀목이 되어주는 사랑하는 동생 보광이, 며느리에게 물심양면으로 지원과 응원을 해 주신 시부모님이 안 계셨다면 박사 과정을 무사히 마치기 힘들었을 것입니다. 가족들의 건강을 기원하며 감사의 인사를 드립니다.

더불어 무사히 대학원 박사 과정에 진학하고 수료까지 할 수 있도록 도와주신 서울아산병원 호흡기내과 교수님들께도 감사의 인사를 드립니다.

지면으로 미처 언급하지 못했지만 저를 아끼고 격려해 주셨던 모든 분들께도 진심으로 감사드립니다. 박사 과정을 통하여 학문의 길로 한 발짝 더 들어선만큼, 앞으로 더욱 정진하고 매진하겠습니다

Abstract

Background: Lung cancer is the most frequently diagnosed cancer and the leading cause of death from cancer worldwide. Lung microbiota have emerged as key modulators of the carcinogenic process. We aimed to evaluate the microbial composition of the lung cancer and adjacent normal lung tissues, investigate the association between lung microbiome and cancer prognosis, and predict the functional profiles of microbiome.

Methods: 216 frozen lung tissues (162 cancer and 54 adjacent normal tissues) which were surgically resected from the patients with lung cancer between January 2018 and December 2019 at Asan Medical Center were retrospectively and randomly selected. The medical records of lung cancer patients were retrospectively reviewed and 16s rRNA gene sequencing was performed. The obtained sequence data were further analyzed by bioinformatics methods.

Results: Cancer group had significantly lower alpha diversity than normal group and microbial composition differed according to histologic type and genetic mutation of cancer. Genus *Romboutsia*, *Christensenellaceae R-7 group*, *Novosphingobium*, *Acinetobacter*, *Rhizobium*, and *Prevotella* were significantly over-represented in cancer group compared with normal group, with some of them occurring more frequently than predicted by the neutral community model. Microbial compositional difference was noted according to postoperative lung cancer stage and the presence of recurrence. In addition, we found several inferred metagenomic functional pathways enriched in different histologic type of lung cancer.

Conclusion: We demonstrated the microbial compositional difference of lung cancer and predicted the metabolic function of lung cancer microbiome. These findings suggested that the altered microbial composition in lung cancer might be associated with cancer initiation and/or progression.

Keywords: Lung cancer, normal lung tissue, microbiome, 16S rRNA

Graphical abstract

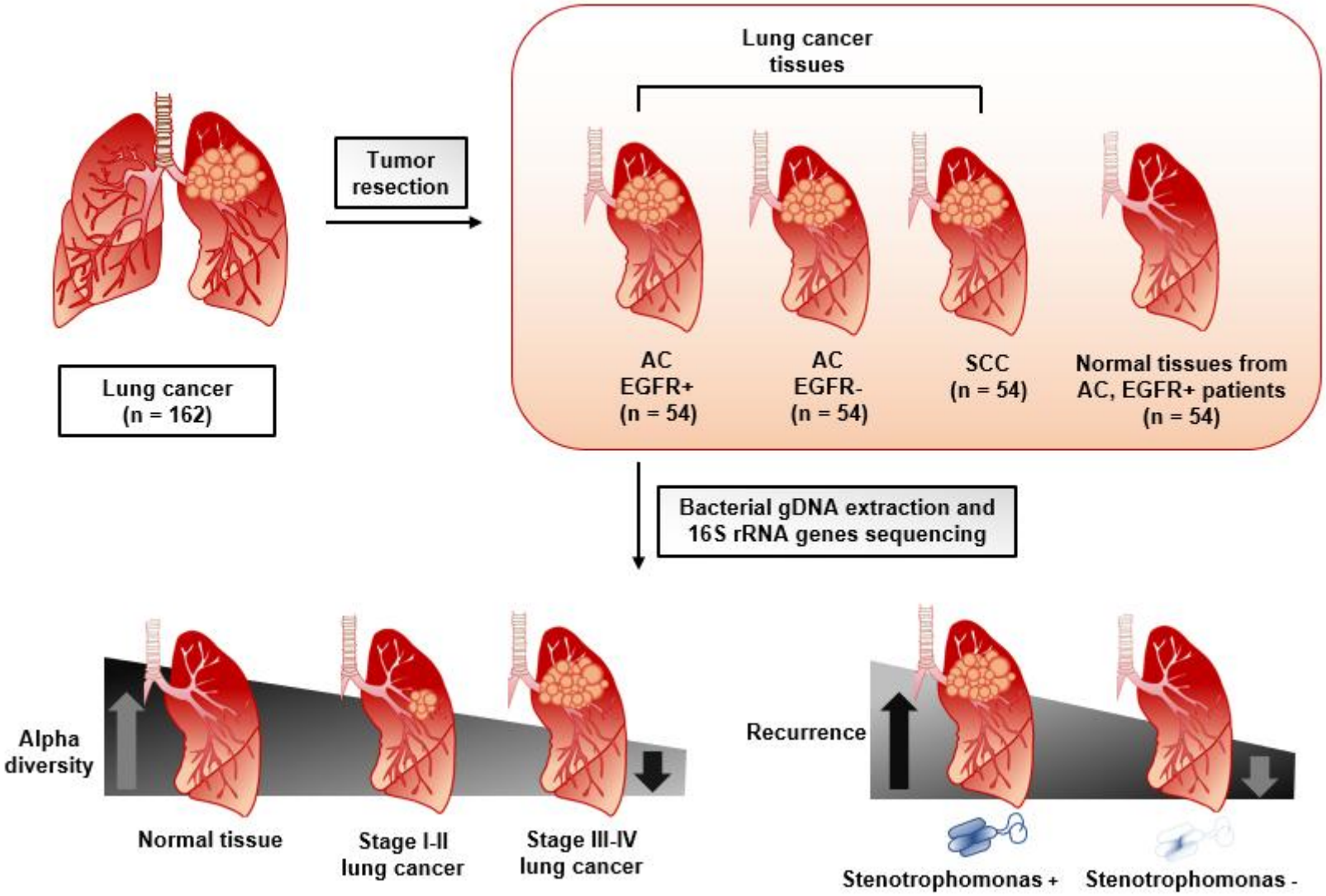

Contents

Tables

Figures

Introduction

Lung cancer is the most frequently diagnosed cancer and the leading cause of death from cancer worldwide, with approximately 11.6% of all cancer diagnoses and 18.4% of all cancer deaths in 2020 [1]. Lung cancer has been widely considered to be a complicated disease caused by interactions between host and environmental factors [2]. Among diverse environmental risk factors, microbiota have emerged as key modulators of both the carcinogenic process and the immune response against cancer cells [3]. While the healthy lung tissues were historically considered as a sterile environment, it has been suggested recently that there were certain microbial species existed in the lung tissues and alterations in the lung microbiome is associated with various lung diseases including lung cancer [4]. Microbiome can contribute to carcinogenesis by host inflammatory pathways induction, bacterial metabolite signaling and genotoxic pathways [4].

Previous studies on lung cancer microbiome have identified phyla *Firmicutes*, *Proteobacteria*, and *Bacteroidetes* including genus *Streptococcus*, *Neisseria*, and *Prevotella* in lung cancer tissues [2, 5-10]. A study by Yu et al. found that genus *Thermus* is more abundant in tissue from advanced stage lung cancer patients and *Legionella* is higher in patients who develop metastases, suggesting their role in tumor progression [8]. Another study showed that greater abundance of families *Bacteroidaceae*, *Lachnospiraceae*, and *Ruminococcaceae* of paired normal lung tissue were associated with reduced recurrence-free or disease-free survival and demonstrated a potential relationship between the normal lung microbiota and lung cancer prognosis [10].

Although studies on lung cancer microbiome are growing rapidly, little is known about microbiota profile in lung cancer tissue, especially, the difference of microbial composition according to histologic type and/or genetic mutation, and the relationship between the microbiome of resected lung cancer tissue and cancer prognosis. In addition, there has been few studies of functional microbiomic approaches (e.g., metagenome, metatranscriptome and metabolome) focused on the metabolic activity and function of the lung microbiota.

Therefore, using 16S rRNA gene sequencing, we aimed to compare the microbial composition of the lung cancer grouped by histologic type and genetic mutation as well as adjacent normal lung tissues, investigate the association between lung microbiome and prognosis of lung cancer and predict the functional profiles from 16S rRNA data.

Methods

Study population and sample collection

We retrospectively and randomly selected 216 frozen lung tissues (162 cancer and 54 adjacent normal tissues) which were surgically resected from the patients with lung cancer between January 2018 and December 2019 at Asan Medical Center. Lung cancer was divided into three groups according to histologic type and the presence of epidermal growth factor receptor (EGFR) mutation: adenocarcinoma with EGFR mutation (AC, EGFR+), adenocarcinoma without EGFR mutation (AC, EGFR-), and squamous cell carcinoma (SCC). 54 cancer tissues were enrolled in each group and paired normal lung tissues were obtained from AC, EGFR+ patients who were predicted to show relatively homogenous features (**Figure 1**). All study patients were consented for collection of frozen tissues in the operating room at the time of their resection. Tissue samples were sterilely cut at the operating room table, transferred to cryovials, and immediately snap frozen in liquid nitrogen. Samples had been stored in Bio-Resource Center at Asan Medical Center until use.

Clinical data including baseline demographics, smoking status, postoperative stage, recurrence, and death were retrospectively collected from medical records in October 2020. The study protocol was approved by the Institutional Review Board of Asan Medical Center (IRB No. 2020-0194).

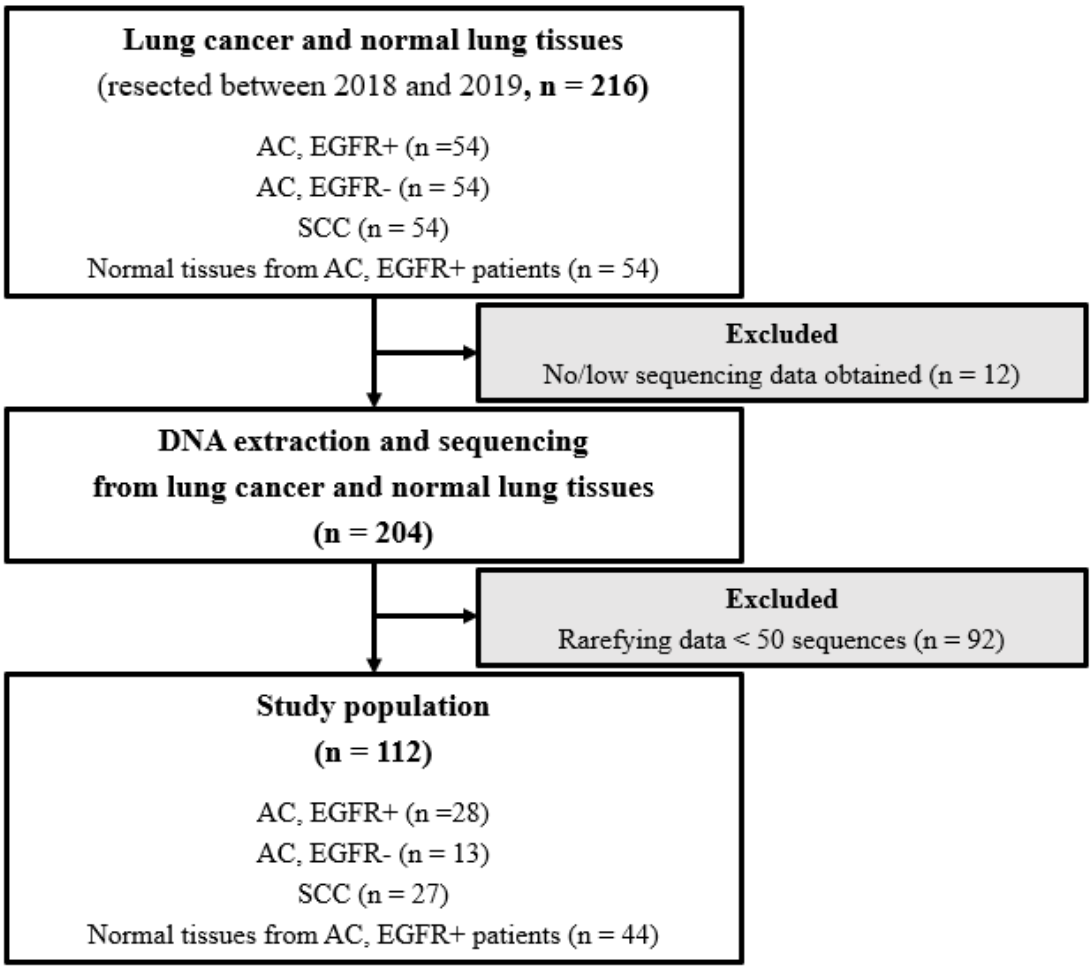

Figure 1. Study flow

DNA extraction and bacterial 16S rRNA genes sequencing

We performed bacterial gDNA extraction process with 216 samples of 54 samples each in a total of four groups (AC, EGFR+; AC, EGFR-; SCC; Normal tissues from AC, EGFR+ patients). DNA extraction was performed with DNeasy PowerSoil Kit (Qiagen, Hilden, Germany) following the manufacture's protocol. We cut each lung tissue using a blade with flame sterilization, and a piece of lung tissue was placed in a PowerBead tube. Horizontal vortexing was conducted with Vortex-Genie 2 (Scientific Industries, Bohemia, New York, USA) at maximum speed. The concentration of gDNA was measured by NanoDrop 2000 spectrophotometer (Thermo Fisher Scientific Inc., Waltham, MA, USA). The polymerase chain reaction (PCR) amplification was performed using the primer that targeted the V4-V5

region of the 16S rRNA (forward: 5'-TCG TCG GCA GCG TCA GAT GTG TAT AAG AGA CAG CCA GCA GCY GCG GTA AN-3'; reverse: 5'-GTC TCG TGG GCT CGG AGA TGT GTA TAA GAG ACA GCC GTC AAT TCN TTT RAG T-3'). The PCR conditions were performed as follows: 95 for 3 minutes for denaturation, 30 cycles of amplification (95 for 30 seconds, 55 for 30 seconds, and 72 for 1 minute). The PCR products were purified using AMPure XP beads (Beckman Coulter, High Wycombe, UK). The quality of the final purified product was measured by the Nanodrop 2000 spectrophotometer. The final products were sequenced using the Illumina Miseq™ platform (Illumina, San Diego, CA, USA).

Microbiome data analysis

Lung tissue microbiome sequences were analyzed using the QIIME™ 2 (Quantitative Insights Into Microbial Ecology) pipeline (2019.7) [11]. The primer sequences of raw sequences were removed by Cutadapt [12] plugin. In this step, reads that included no bacterial primer sequences or a low-quality primer sequences were removed. We denoised the sequences using dada2 plugin implemented in QIIME™ 2, and bacterial amplicon sequence variants (ASVs) were identified. The ASVs were classified using the SILVA database [13]. Chloroplastic and mitochondrial, and unassigned ASVs were filtered by using taxa filter. We aligned the ASVs using the phylogeny align-to-tree-mafft-fasttree plugin, and microbial diversity analyses were performed with rarefying samples to an even depth of 50 sequences per sample.

Alpha diversity was evaluated by Chao1, Shannon index and phylogenetic diversity [14, 15]. Beta diversity was assessed using unweighted UniFrac distances [16]. Microbial compositional differences between different groups were visualized by principal coordinates analysis (PCoA). Unweighted intra-group UniFrac distances between each sample and all other samples from the same group were represented by box-and-whiskers plots. Differential taxonomy was identified by linear discriminant analysis (LDA) effect size (LEfSe) [17]. We used the neutral community model-based dominance test to determine the cause of the difference in lung microbiome between the normal and cancer groups [18]. Additionally, we conducted a stratified sub-analysis by the postoperative stage and the recurrence of lung cancer to address the association between lung microbiome and the prognosis of lung cancer [10]. Phylogenetic

Investigation of Communities by Reconstruction of Unobserved States 2 (PICRUSt2) v.2.1.3-b software which predicts gene family abundance was used for predicting the functional profiles from 16S rRNA data [19, 20]. The ASV table from bacterial community analysis and representative sequences were used, and predicted functional profiles were gained using the picrust2_pipeline.py. We used MetaCyc pathway that was inferred through PICRUSt2.

Statistical analyses

All clinical data are presented as mean ± standard deviation or median (interquartile range [IQR]) for continuous variables, and numbers (%) for categorical variables. Data categorized according to cancer types were compared using the One-way ANOVA or the Kruskal-Wallis test (for continuous variables) and the χ^2 or the Fisher's exact test (for categorical variables). If there was a significant difference among the three values, a *post hoc* analysis for multiple comparisons was performed with the application of Bonferroni correction. All analyses for clinical data were performed using the SPSS software (Version 24.0; SPSS, Chicago, IL, USA).

We conducted an analysis of similarity (ANOSIM) to identify differential microbial community. To see any significant difference in alpha diversity and the UniFrac dissimilarities, we performed the Wilcoxon rank-sum test, or t-test in R. Kruskal-Wallis rank-sum test was used to distinguish significant differential abundance among different groups in LEfSE analysis. The Kaplan-Meier method was used to estimate the cumulative rate of recurrence. All significance tests were two-sided and p-values <0.05 were considered to indicate statistical significance.

Results

Clinical characteristics of study population

The mean patient age was 65.3 years, with a preponderance of men (64.8%). Comparing into three groups according to cancer types, the proportions of male gender and smokers were significantly greater in the SCC group than in the AC, EGFR+ and AC, EGFR- group ($p<0.001$, respectively). In addition, the SCC group had a significantly higher median number of pack years (39 pack-years) compared with other groups ($p<0.001$). Otherwise, there were no significant differences in age, postoperative stage, nodal stage, recurrence, and death between the three groups. **Table 1** presents the clinical characteristics of the 162 study patients.

Table 1. Clinical characteristics of study population

	AC, EGFR+ (n = 54)	AC, EGFR- (n = 54)	SCC (n = 54)	p-value			
					AC, EGFR+ *vs.* AC, EGFR-	AC, EGFR- *vs.* SCC	SCC *vs.* AC, EGFR+
Age, yr	64.9 ± 9.3	64.2 ± 9.2	66.7 ± 9.4	0.358			
Male gender, n (%)	28 (51.9%)	25 (46.3%)	52 (96.3%)	<0.001	0.564	<0.001	<0.001
Body mass index (kg/m^2)	25.0 ± 2.5	25.0 ± 3.4	24.7 ± 3.0	0.882			
Smoking status							
Non-smoker, n (%)	30 (55.6%)	31 (57.4%)	3 (5.6%)	<0.001	0.846	<0.001	<0.001
Ever smoker, n (%)	24 (44.4%)	23 (42.6%)	51 (94.4%)				
Pack-years, median (IQR)	0 (0–30)	0 (0–27)	39 (20–46)	<0.001	0.671	<0.001	<0.001
Stage, n (%)							
–	41 (75.9%)	44 (81.5%)	45 (83.3%)	0.603			
–	13 (24.1%)	10 (18.5%)	9 (16.7%)				
Nodal stage							
N0	39 (72.2%)	45 (83.3%)	39 (72.2%)	0.296			
N1-2	15 (27.8%)	9 (16.7%)	15 (27.8%)				
Follow-up duration months, median (IQR)	27.5 (24.0–29.0)	22.0 (18.8–25.3)	25.0 (11.8–27.0)	<0.001	<0.001	0.193	0.004
Recurrence, n (%)	16 (29.6%)	13 (24.1%)	9 (16.7%)	0.280			
Death, n (%)	2 (3.7%)	1 (1.9%)	6 (11.1%)	0.085			

Microbial diversity and taxonomy

The lung tissue microbiome of 216 tissues were analyzed by 16S rRNA gene amplicon sequencing. The 12 samples that had no or low sequencing data were excluded. In 204 samples, a total of 8,671,731 paired-end reads was merged into 329,528 reads from the tissue samples and an average of 1,525 merged reads per sample. As the rarefied depth was 50, we calculated the alpha diversity and beta diversity with 112 samples (**Figure 1**).

Alpha diversity indexes including Chao1, Shannon, and phylogenetic diversity were significantly higher in the normal group than in the cancer group ($p<0.0001$, $p<0.05$, and $p<0.01$, respectively, **Figure 2A**). When compared by dividing into three groups according to histologic type of cancer, Chao1 and phylogenetic diversity were higher in the normal group than in the AC and SCC groups (**Figure 2B**). Comparison among the four groups in accordance with the histologic type and EGFR mutation showed that the normal group had greater diversity than all other types of cancer group, as assessed by Chao1 index (**Figure 2C**).

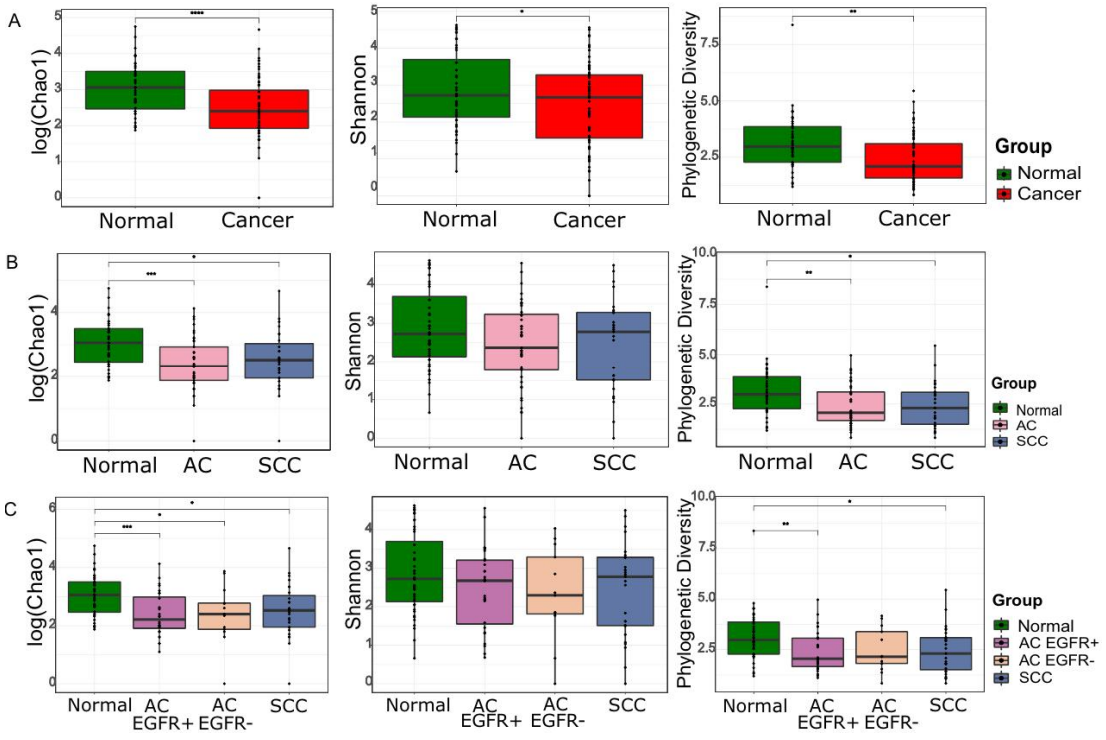

Figure 2. Comparison of alpha diversity indexes (Chao1, Shannon, and phylogenetic diversity) between lung cancer and normal lung tissues

(A) Normal vs. Cancer, (B) Normal vs. AC vs. SCC, and (C) Normal vs. AC, EGFR+ vs. AC, EGFR- vs. SCC. Box plot represented the minimum, first quartile, median, third quartile, and maximum of alpha indexes.

When we performed sub-analysis by rarefying samples to the depth of 25 and 100 sequences according to the study flow of **Figure 3**, not only Chao1 index but also phylogenetic diversity was greater in the normal group than all other types of cancer group (**Figure 4**).

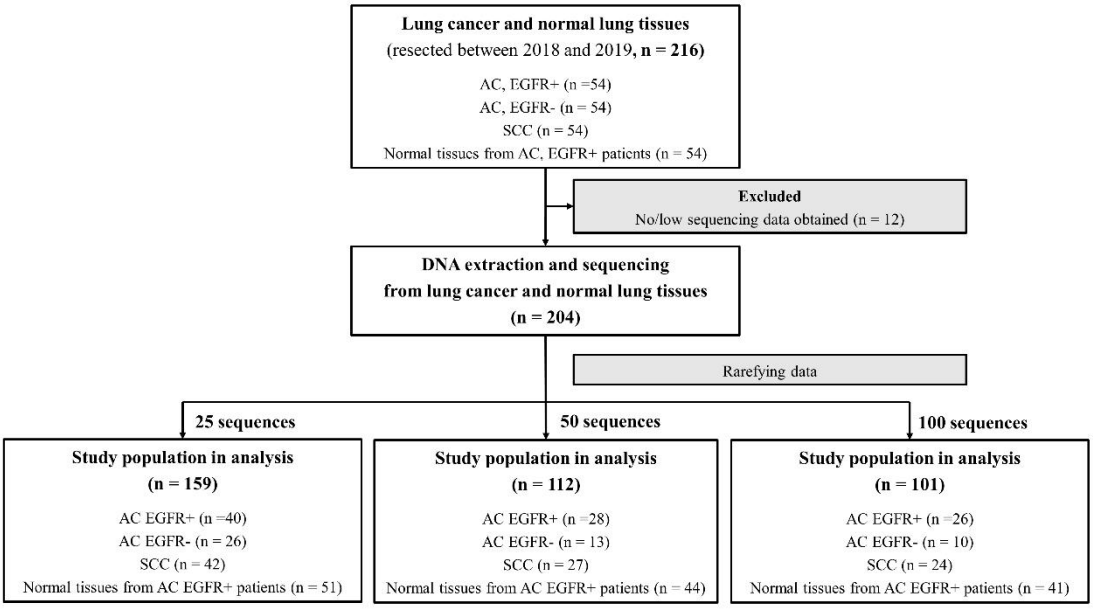

Figure 3. Study flow as rarefying samples at various sequences

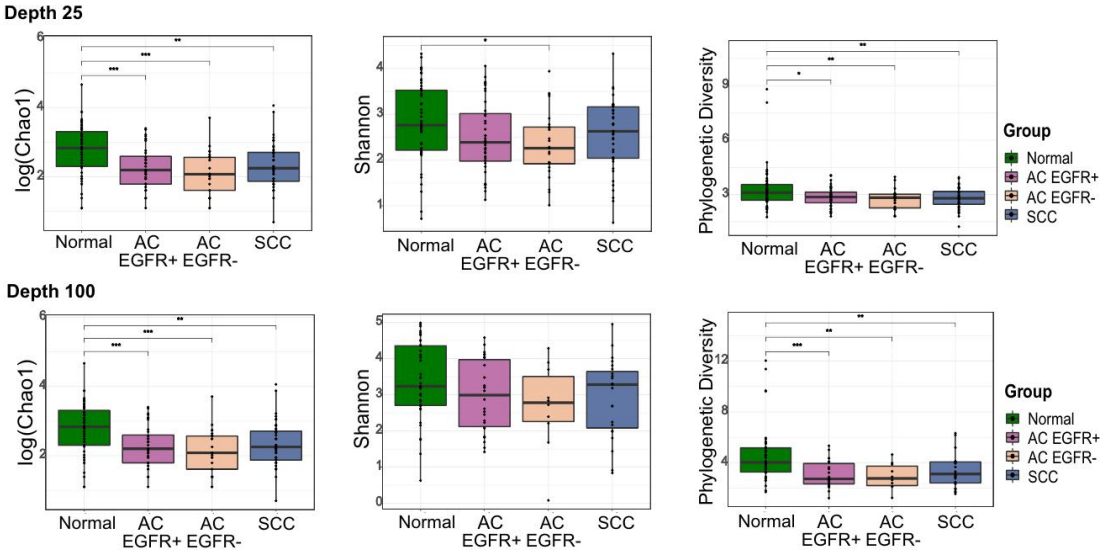

Figure 4. Comparison of alpha diversity between lung cancer and normal lung tissues by rarefying samples to the depth of 25 and 100 sequence

To evaluate the similarity of microbiota profiles, unweighted UniFrac distances were calculated. The PCoA based on the unweighted UniFrac distance revealed significant compositional differences between different groups, indicating more heterogeneity of the microbial distribution in the cancer group (**Figure 5B and 5C**). The result was similar in sub-analysis where samples were rarefied to the depth of 25 and 100 sequences (**Figure 6**). Among the cancer groups, there was also a compositional difference between AC and SCC (**Figure 5D**).

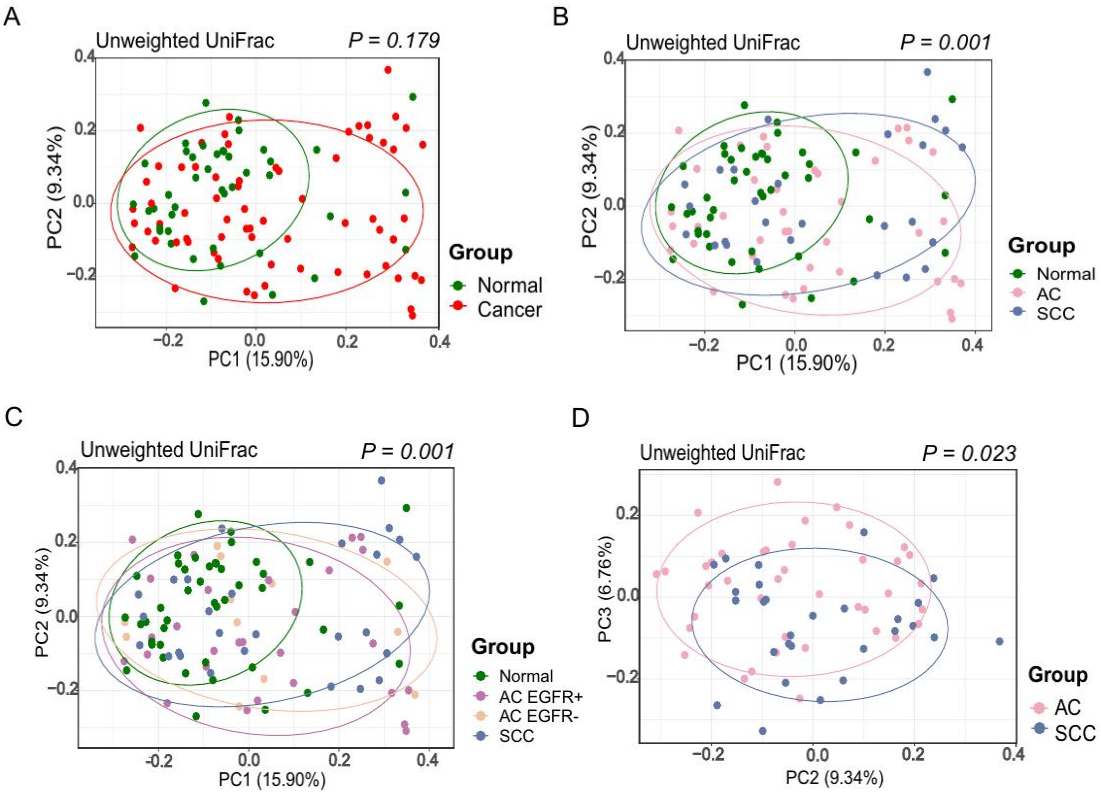

Figure 5. Principal coordinates analyses of the unweighted UniFrac distance between different groups. (A) Normal vs. Cancer, (B) Normal vs. AC vs. SCC, (C) Normal vs. AC, EGFR+ vs. AC, EGFR- vs. SCC, and (D) AC vs. SCC.

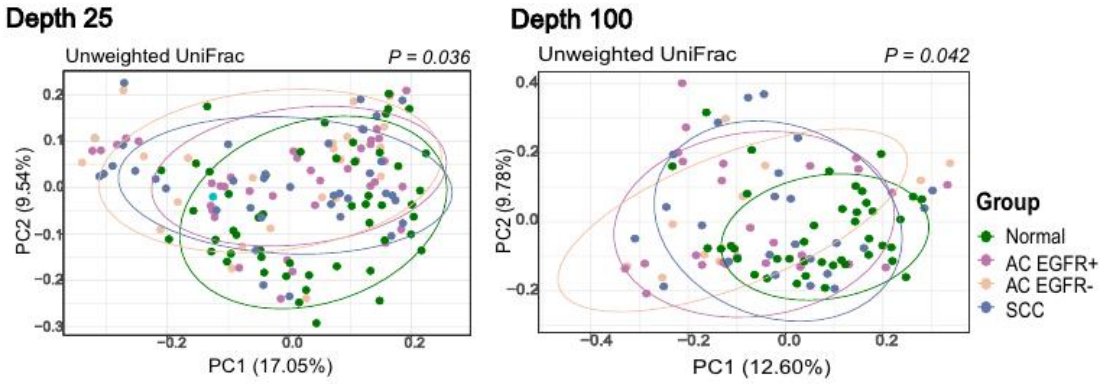

Figure 6. Comparison of beta diversity between lung cancer and normal lung tissues by rarefying samples to the depth of 25 and 100 sequence

The Box-and-whisker plot of unweighted intra-group UniFrac distance showed that cancer group had a significantly greater dissimilarity among the samples than normal group, especially as the order of SCC, AC and normal group (**Figure 7)**.

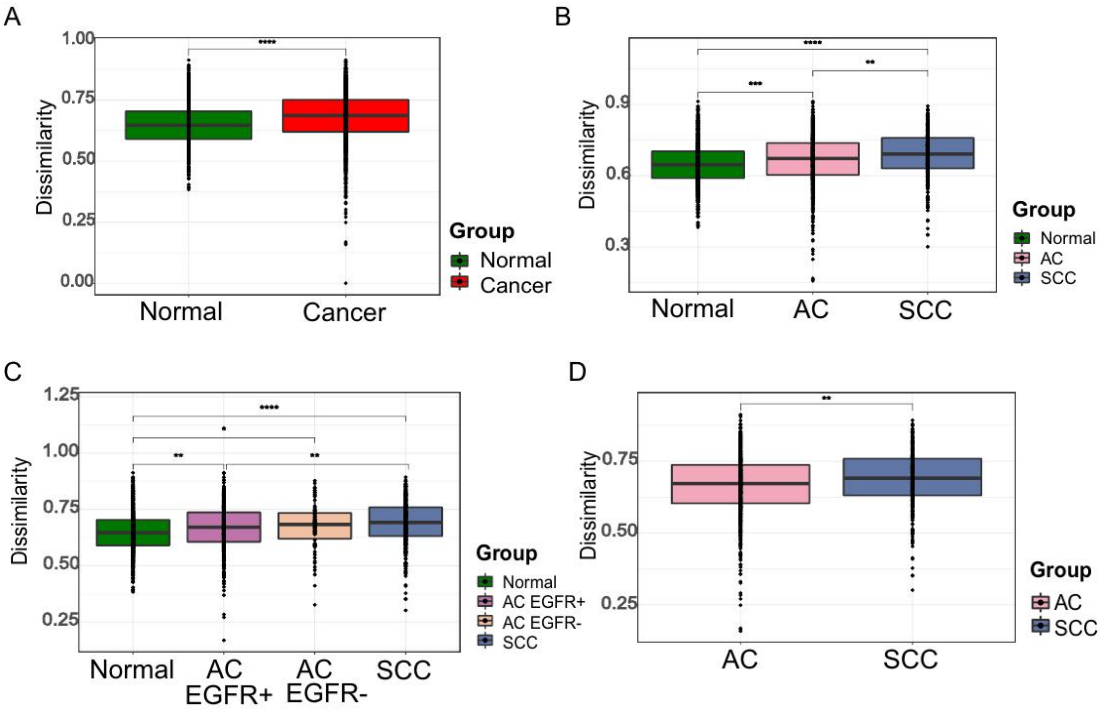

Figure 7. Box-and-whisker plot of unweighted intra-group UniFrac distance between each sample and all other samples from the same group. (A) Normal vs. Cancer, (B) Normal vs. AC vs. SCC, (C) Normal vs. AC, EGFR+ vs. AC, EGFR- vs. SCC, and (D) AC vs. SCC.

To detect taxa with differential abundance among different groups, we used LEfSe with LDA values of 3.0. In comparison of cancer and normal group, 25 bacterial taxa at genus level with significant abundance differences were identified. Genus *Romboutsia*, *Christensenellaceae R-7 group*, *Novosphingobium*, *Acinetobacter*, *Rhizobium*, and *Prevotella* were significantly over-represented in cancer group and a number of other taxa including *Staphylococcus*, *Lactobacillus*, and *Bacteroides* were enriched in normal group. Taxa enriched in different groups are displayed in **Figure 8**.

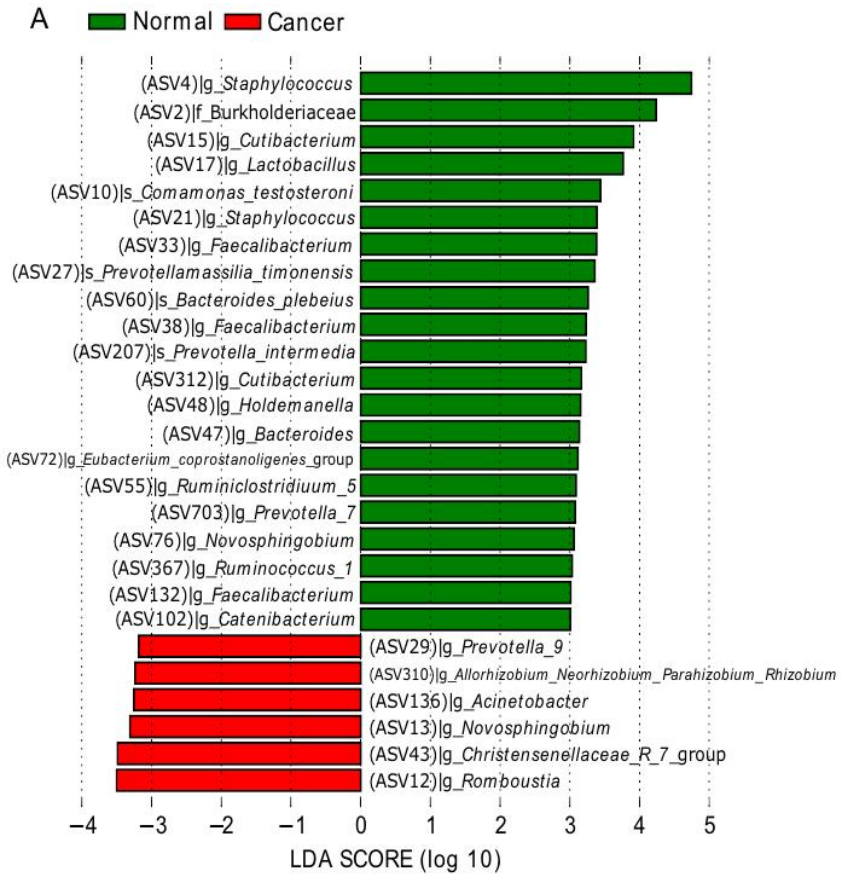
A
Normal
Cancer
(ASV4)|g_Staphylococcus
(ASV2)|f_Burkholderiaceae
(ASV15)|g_Cutibacterium
(ASV17)|g_Lactobacillus
(ASV10)|s_Comamonas_testosteroni
(ASV21)|g_Staphylococcus
(ASV33)|g_Faecalibacterium
(ASV27)|s_Prevotellamassilia_timonensis
(ASV60)|s_Bacteroides_plebeius
(ASV38)|g_Faecalibacterium
(ASV207)|s_Prevotella_intermedia
(ASV312)|g_Cutibacterium
(ASV48)|g_Holdemanella
(ASV47)|g_Bacteroides
(ASV72)|g_Eubacterium_coprostanoligenes_group
(ASV55)|g_Ruminiclostridiuum_5
(ASV703)|g_Prevotella_7
(ASV76)|g_Novosphingobium
(ASV367)|g_Ruminococcus_1
(ASV132)|g_Faecalibacterium
(ASV102)|g_Catenibacterium
(ASV29)|g_Prevotella_9
(ASV310)|g_Allorhizobium_Neorhizobium_Parahizobium_Rhizobium
(ASV136)|g_Acinetobacter
(ASV13)|g_Novosphingobium
(ASV43)|g_Christensenellaceae_R_7_group
(ASV12)|g_Romboustia
−4 −3 −2 −1 0 1 2 3 4 5
LDA SCORE (log 10)

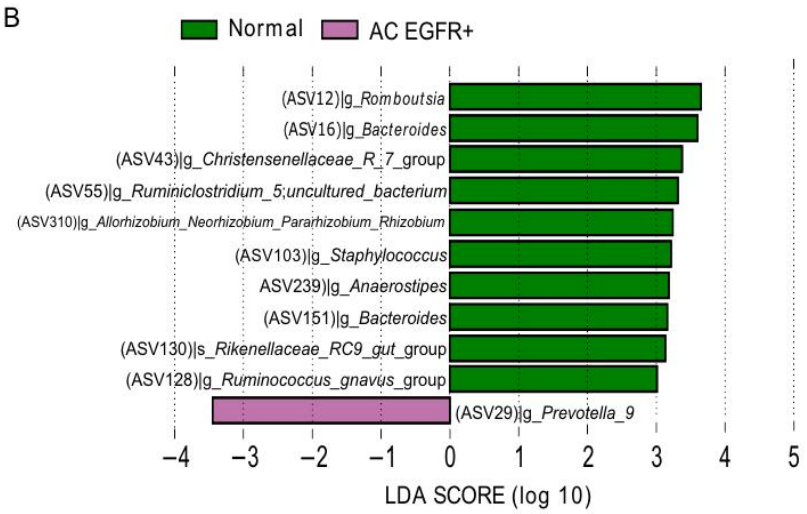
B
Normal
AC EGFR+
(ASV12)|g_Romboutsia
(ASV16)|g_Bacteroides
(ASV43)|g_Christensenellaceae_R_7_group
(ASV55)|g_Ruminiclostridium_5;uncultured_bacterium
(ASV310)|g_Allorhizobium_Neorhizobium_Parahizobium_Rhizobium
(ASV103)|g_Staphylococcus
ASV239)|g_Anaerostipes
(ASV151)|g_Bacteroides
(ASV130)|s_Rikenellaceae_RC9_gut_group
(ASV128)|g_Ruminococcus_gnavus_group
(ASV29)|g_Prevotella_9
−4 −3 −2 −1 0 1 2 3 4 5
LDA SCORE (log 10)

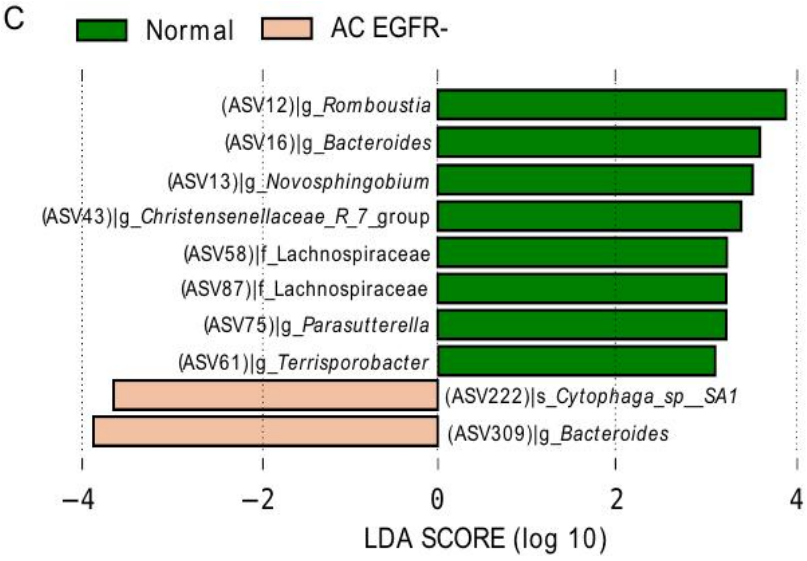
C
Normal
AC EGFR-
(ASV12)|g_Romboustia
(ASV16)|g_Bacteroides
(ASV13)|g_Novosphingobium
(ASV43)|g_Christensenellaceae_R_7_group
(ASV58)|f_Lachnospiraceae
(ASV87)|f_Lachnospiraceae
(ASV75)|g_Parasutterella
(ASV61)|g_Terrisporobacter
(ASV222)|s_Cytophaga_sp__SA1
(ASV309)|g_Bacteroides
−4 −2 0 2 4
LDA SCORE (log 10)

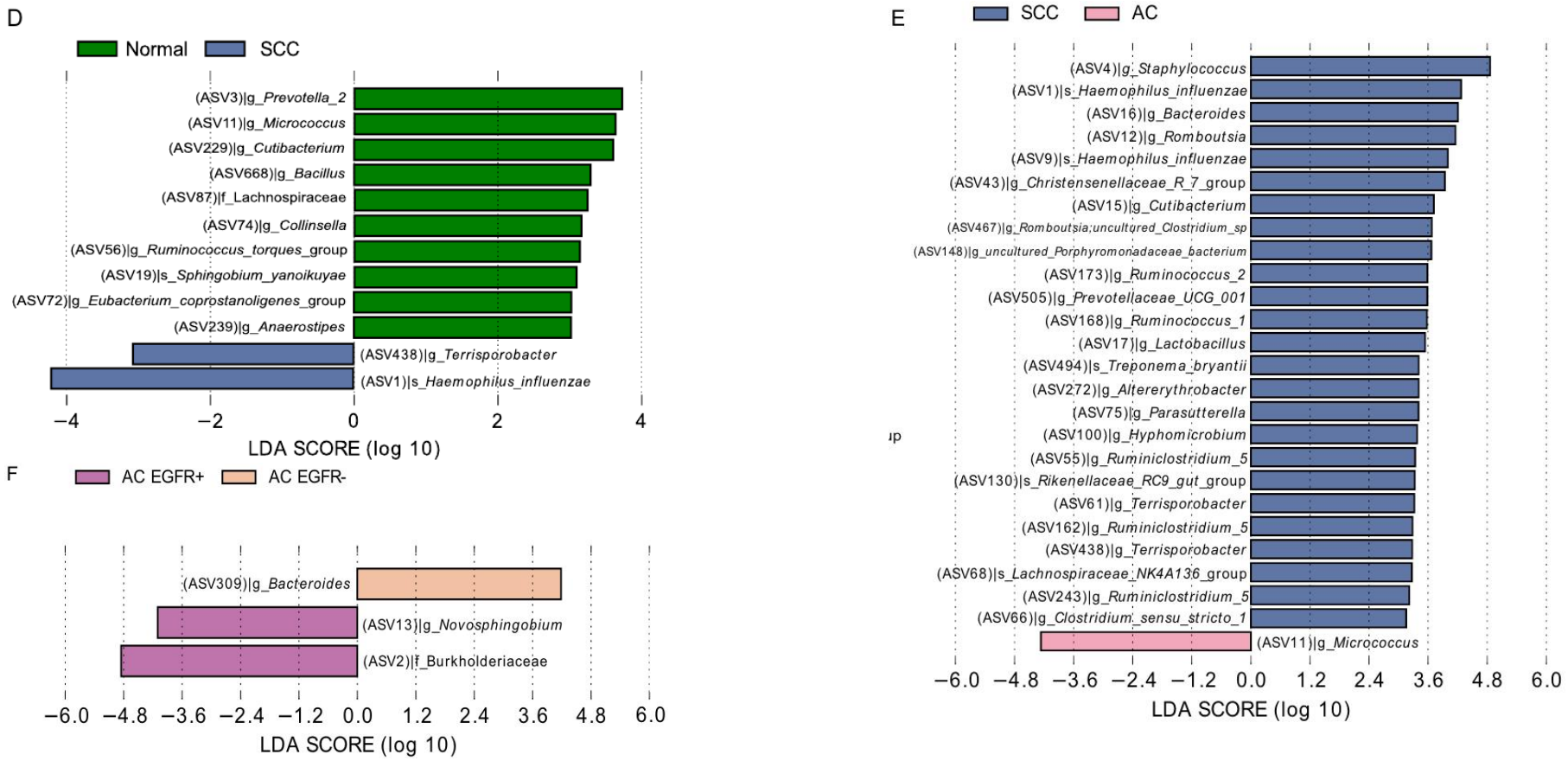

Figure 8. The linear discriminant analysis effect size plots of bacterial communities in cancer and normal lung tissues. Linear discriminant analysis scores were calculated, with higher scores indicating greater effect size (significance determined by LDA score >3.0 and $p<0.05$ for Kruskal-Wallis rank-sum test). Taxonomic categories include f = family, g = genus, and s = species. (A) Normal vs. Cancer, (B) Normal vs. AC, EGFR+, (C) Normal vs. AC, EGFR-, (D) Normal vs. SCC, (E) SCC vs. AC, and (F) AC, EGFR+ vs. AC. EGFR-.

Notably, species *Haemophilus influenzae* (*H. influenzae*) was enriched in SCC group compared with normal group (**Figure 8D**). In total, four ASVs were classified as species *H. influenzae* and there were nine samples containing those ASVs. Seven of them (77.8%, 7/9) were in SCC group, one in normal group and the other in AC group. **Table 2** presents the count of ASVs classified as species *H. influenzae* in each sample.

Table 2. The count of ASVs classified as species *H. influenzae* in each sample

Group	Patient age/sex	ASV1	ASV9	ASV24	ASV1011
Normal	80/F	0	0	0	5
AC	58/F	225	0	0	0
SCC	72/M	796	4008	820	0
SCC	71/M	6	0	0	0
SCC	67/M	0	15	0	0
SCC	66/M	3	0	0	0
SCC	83/M	0	54	0	0
SCC	71/F	29116	0	0	0
SCC	59/M	6	0	0	0

We reviewed the clinical data of seven SCC patients whose lung tissue samples had species *H. influenzae*. The mean age of them was 69.9 years and 85.7% were men. All of them were ever smokers with a median of 40 pack years smoking history. Among them, 85.7% (6/7) had used antibiotics within 3 months of the date of tissue collection. The clinical characteristics of the SCC patients with *H. influenzae* in their cancer tissues were presented in **Table 3**.

Table 3. Clinical characteristics of the SCC patients with *H. influenzae* in their cancer tissues

	SCC patients with *H. influenzae* in their cancer tissues (n = 7)
Age, yr	69.9 ± 7.3
Male gender, n (%)	6 (85.7%)
Body mass index (kg/m^2)	26.0 ± 4.4
Smoking status	
Past smoker, n (%)	6 (85.7%)
Current smoker, n (%)	1 (14.3%)
Pack-years, median (IQR)	40 (30–40)
Stage, n (%)	
–	5 (71.4%)
–	2 (28.6%)
Nodal stage	
N0	5 (71.4%)
N1-2	2 (28.6%)
Recurrence, n (%)	4 (14.3%)

Then, we selected two SCC tissues with the most abundant *H. influenzae* ASVs. The tissues were disrupted with stainless steel beads, plated and cultured on Chocolate agar in 5% CO2 at 37℃. After three days, we observed colonies in the one of two SCC tissues. We picked the colonies and spread them onto a fresh Chocolate agar plate using a dilution streaking method [21)]. We incubated the plate in 5% CO2 at 37℃ for three days and the colonies have grown up. We could identify *H. influenzae* by 16S rRNA sequencing from the pure culture.

We used the neutral community model-based dominance test to determine the cause of the difference in lung microbiome between the normal and cancer groups (**Figure 9**). The goodness-of-fit (R^2) values were 0.74 with normal group and 0.64 with cancer group, respectively. Considering that R^2 value closure to 1 implies that the composition of the lung microbiome is consistent with neutral processes of dispersal and ecological drfit [18)], the microbial community of normal group was a better fit with the neutral model than that of cancer group. Then, we determined if any ASVs deviated from predictions of the neutral model. While some ASVs including genus *Micrococcus*, *Romboutsia*, *Novosphingobium*, *Bacteroides*,

Parasutterella, and *Sphingobium* were over-represented, species *H. influenzae* and family *Burkholderiaceae* were under-represented in cancer group.

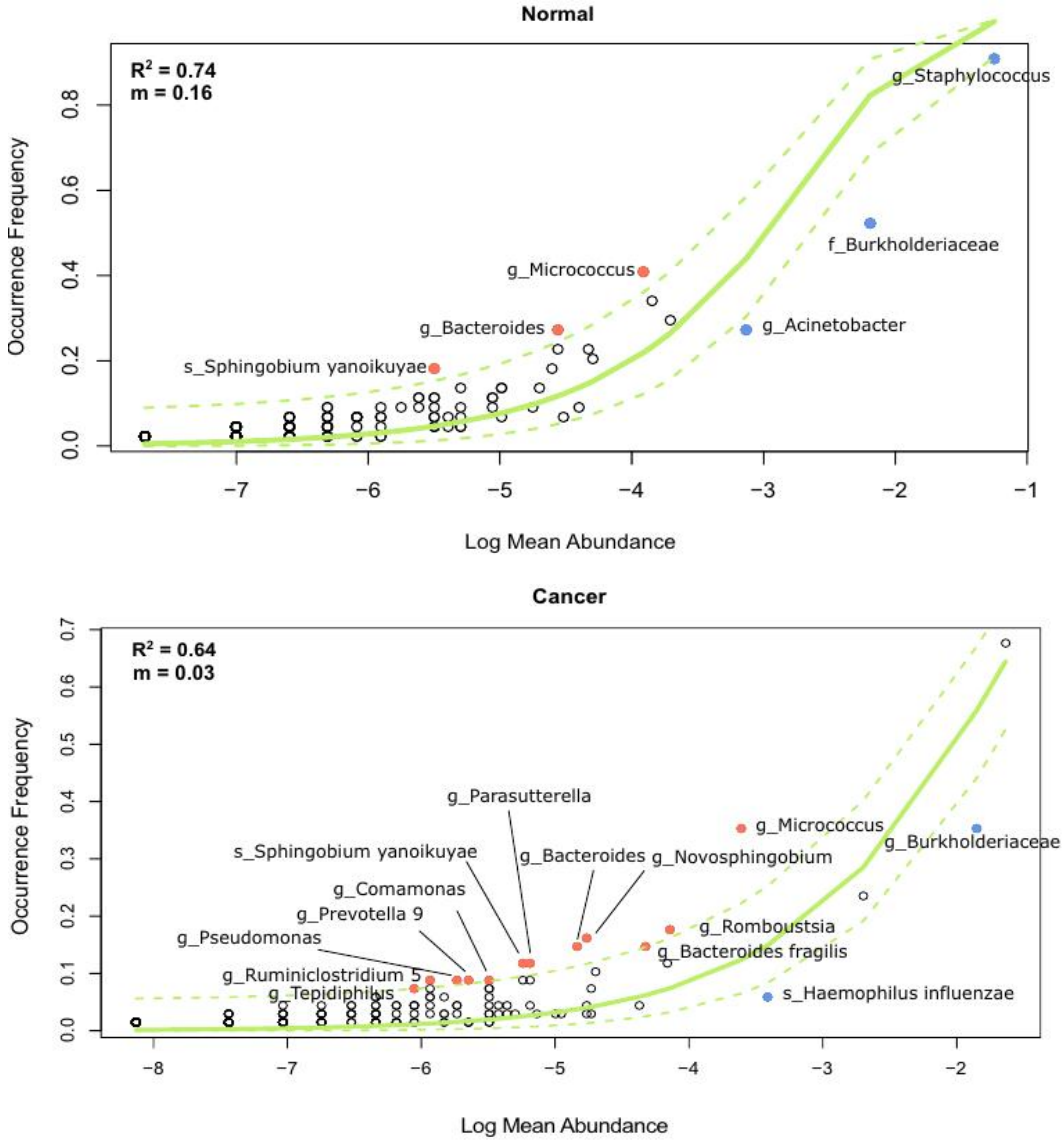

Figure 9. The neutral community model-based dominance analysis

The theoretical and observed relationships between the log mean relative abundance of a species and the occurrence frequency were compared. Each dot represents a different amplicon sequence variant (ASV) and the solid green line represents the best fit to the neutral mode. Dashed lines indicate 95% confidence intervals for the neutral model prediction. ASV occurring more frequently than predicted by the model are shown in orange whereas those that occurred less frequently than predicted are shown in blue.

Microbiome analysis as postoperative lung cancer stage

To address the association between lung microbiome and prognosis of lung cancer, microbial diversity and taxonomy were analyzed by dividing cancer group according to the postoperative stage: stage – and stage – of TNM classification. Alpha diversity evaluated by Chao1 and phylogenetic diversity was steadily declined from normal to stage I–II to stage – (**Figure 10A**). Compositional differences were noted based on beta diversity analysis. The PCoA plot revealed that microbial distribution differed along with postoperative lung cancer stage (p = 0.014, **Figure 10B**). Although there was no statistical significance, lung cancer of more advanced stage tended to have a greater dissimilarity among the samples than that of earlier stage. (**Figure 10C**). In the LEfSe analysis of three subgroups according to postoperative lung cancer staging, genus *Staphylococcus*, *Burkholderia-Caballeronia-Paraburkholderia*, and *Peptoniphilus* were enriched in advanced stage lung cancer group (**Figure 10D**). When we compared the relative abundance of genus *Staphylococcus* which was identified as the most predominant ASV in advanced stage lung cancer, there was no significant difference between stage I–II and stage – groups (p = 0.687, **Figure 10E**).

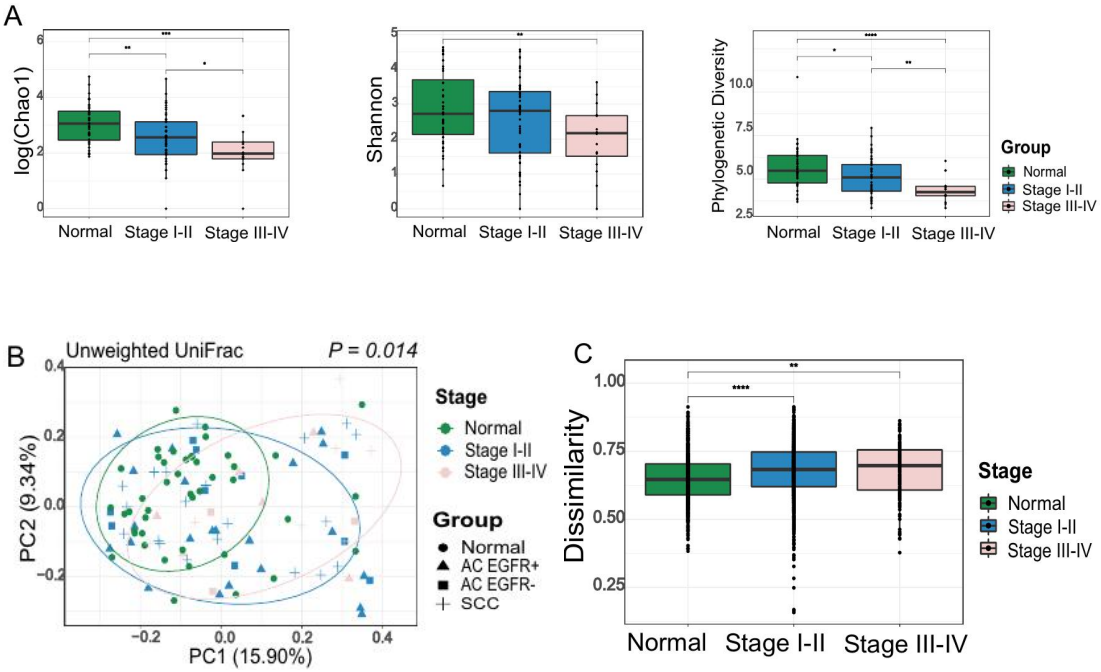

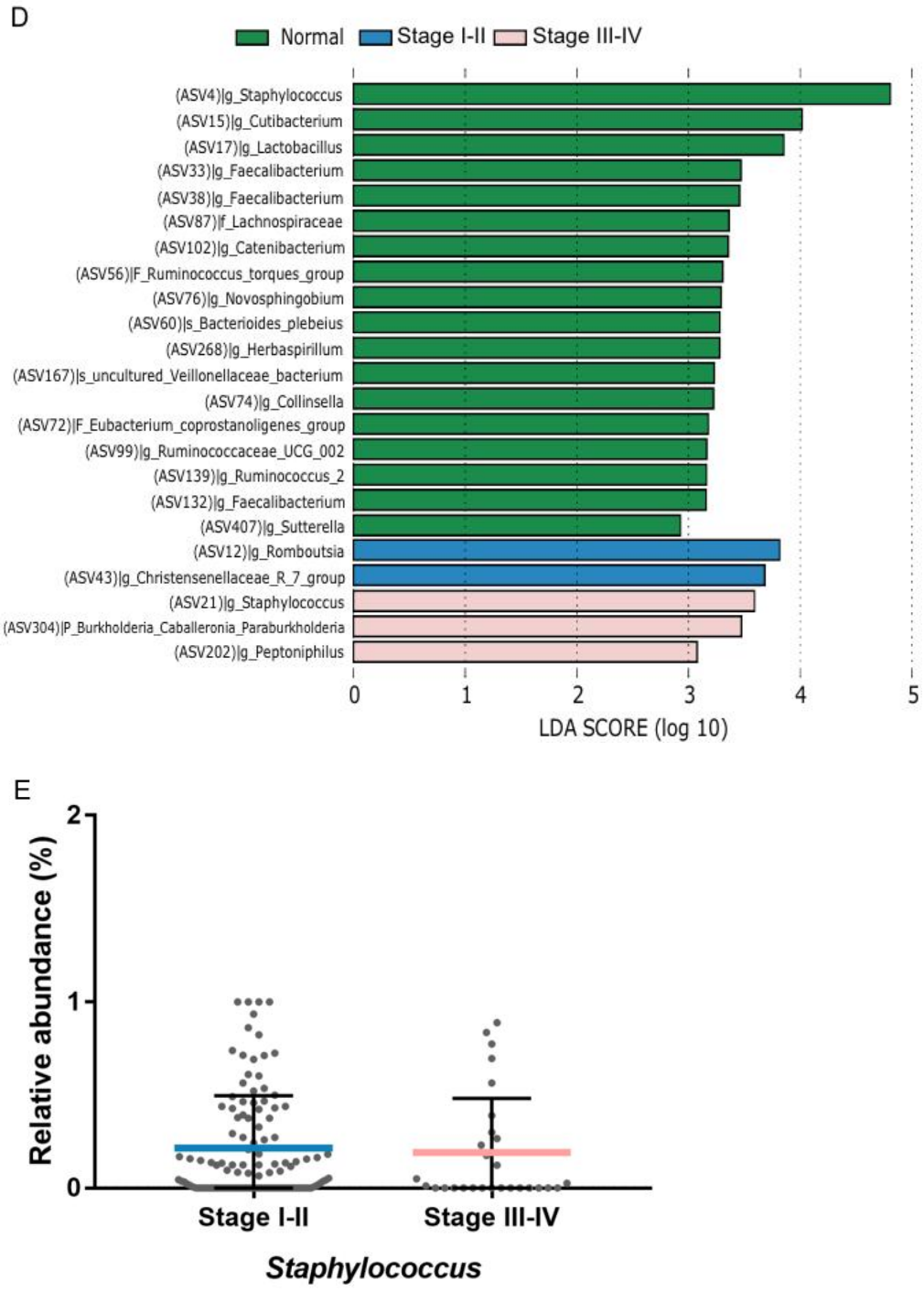

Figure 10. Microbiome analysis as postoperative lung cancer stage

(A) Comparison of alpha diversity indexes (Chao1, Shannon, and phylogenetic diversity), (B) Principal coordinates analyses of the unweighted UniFrac distance, (C) Box-and-whisker plot

of unweighted intra-group UniFrac distance, (D) The LEfSe analysis of bacterial communities, and (E) Comparison of the relative abundance of genus *Staphylococcus*.

Microbiome analysis as the recurrence of lung cancer

Then, we analyzed microbial diversity and taxonomy by dividing cancer group according to the presence of recurrence during follow-up period. Alpha diversity indexes did not differ according to the recurrence (**Figure 11A**). Compositional differences were noted based on beta diversity analysis. The PCoA plot revealed that microbial distribution differed along with the presence of recurrence, presenting more heterogenous microbial distribution in the cancer with recurrence group ($p = 0.002$, **Figure 11B**). Considering the unweighted intra-group UniFrac distance in **Figure 11C**, the dissimilarity among the samples steadily increased, as the order of normal, lung cancer without recurrence and lung cancer with recurrence. In the LEfSe analysis of three subgroups according to the recurrence, several differential microbial taxa including genus *Stenotrophomonas*, *Bacteroides*, and *Peptoniphilus* were noted in the cancer group with recurrence (**Figure 11D**). To estimate the cumulative rate of recurrence according to the presence of genus *Stenotrophomona*s which was identified as the most predominant in lung cancer with recurrence group, we used the Kaplan-Meier method. The cumulative rate of recurrence was significantly higher in the group with *Stenotrophomonas* than in those without *Stenotrophomonas* ($p = 0.013$, **Figure 11E**).

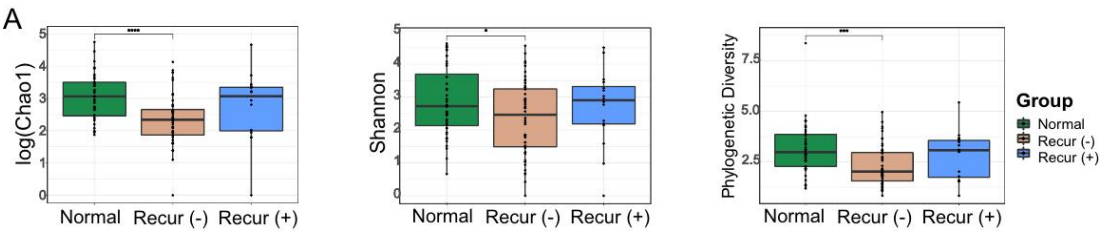

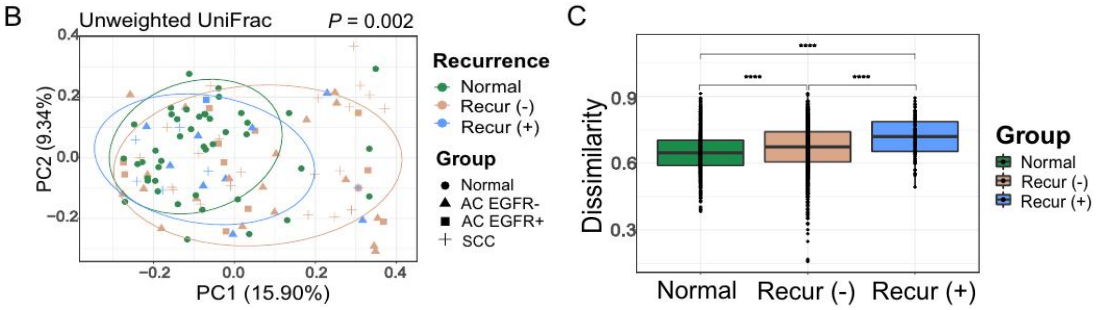
B
Unweighted UniFrac
P = 0.002
PC2 (9.34%)
PC1 (15.90%)
Recurrence
Normal
Recur (-)
Recur (+)
Group
Normal
AC EGFR-
AC EGFR+
SCC
C
Dissimilarity
Normal
Recur (-)
Recur (+)
Group
Normal
Recur (-)
Recur (+)

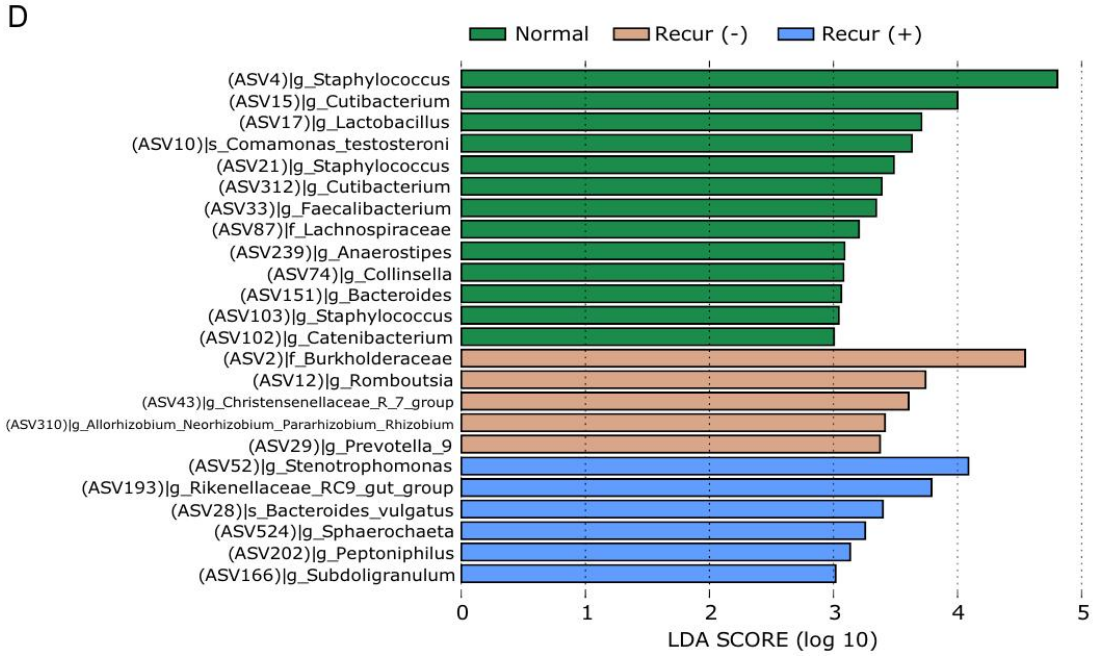
D
Normal
Recur (-)
Recur (+)
(ASV4)|g_Staphylococcus
(ASV15)|g_Cutibacterium
(ASV17)|g_Lactobacillus
(ASV10)|s_Comamonas_testosteroni
(ASV21)|g_Staphylococcus
(ASV312)|g_Cutibacterium
(ASV33)|g_Faecalibacterium
(ASV87)|f_Lachnospiraceae
(ASV239)|g_Anaerostipes
(ASV74)|g_Collinsella
(ASV151)|g_Bacteroides
(ASV103)|g_Staphylococcus
(ASV102)|g_Catenibacterium
(ASV2)|f_Burkholderaceae
(ASV12)|g_Romboutsia
(ASV43)|g_Christensenellaceae_R_7_group
(ASV310)|g_Allorhizobium_Neorhizobium_Pararhizobium_Rhizobium
(ASV29)|g_Prevotella_9
(ASV52)|g_Stenotrophomonas
(ASV193)|g_Rikenellaceae_RC9_gut_group
(ASV28)|s_Bacteroides_vulgatus
(ASV524)|g_Sphaerochaeta
(ASV202)|g_Peptoniphilus
(ASV166)|g_Subdoligranulum
LDA SCORE (log 10)

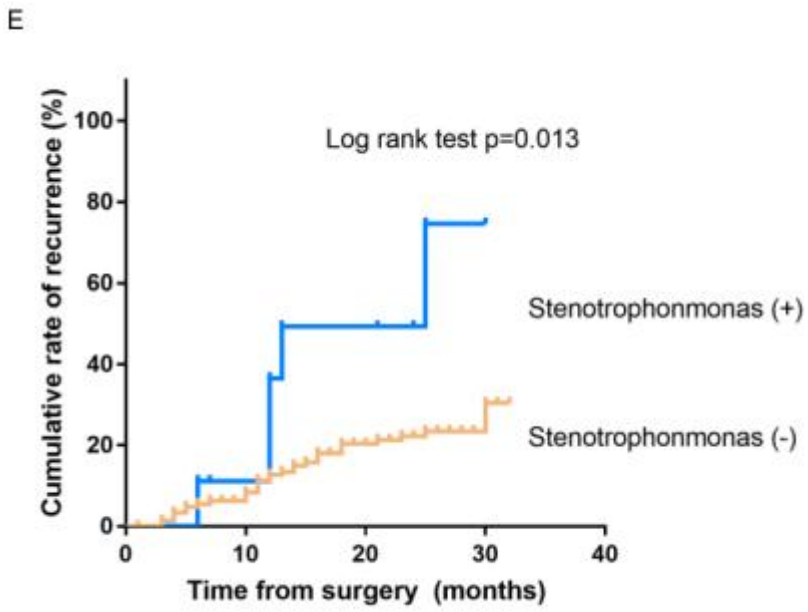
E
Log rank test p=0.013
Cumulative rate of recurrence (%)
Stenotrophonmonas (+)
Stenotrophonmonas (-)
Time from surgery (months)

Figure 11. Microbiome analysis as the recurrence of lung cancer

(A) Comparison of alpha diversity indexes (Chao1, Shannon, and phylogenetic diversity), (B) Principal coordinates analyses of the unweighted UniFrac distance, (C) Box-and-whisker plot of unweighted intra-group UniFrac distance, (D) The LEfSe analysis of bacterial communities, and (E) The cumulative rate of recurrence according to the presence of genus *Stenotrophomona*s.

Pathway analysis predicted by PICRUSt2

To better understand how the bacterial functional profiles differed according to the histologic type of cancer, we used PICRUSt2, a bioinformatics software to predict functional metagenomes from 16S rRNA gene profiling. We found 18 differentially abundant MetaCyc pathways among the three groups (chosen by LDA score > 2.9) (**Figure 12**). The pathways related to tricarboxylic acid (TCA) cycle, sulfur compound metabolism, fatty acid salvage, and L-glutamate and L-glutamine biosynthesis were predominantly found in AC group, whereas those related to adenine and adenosine salvage, acetylene degradation, purine and pyrimidine nucleotide degradation, L-arginine degradation, formaldehyde assimilation, biotin biosynthesis, and 2-carboxy-1, 4-naphthoquinol biosynthesis were predominant in SCC group.

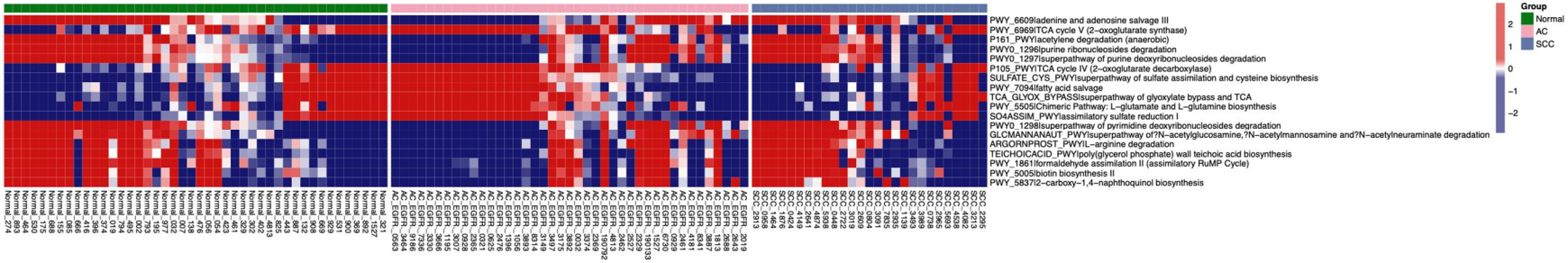

Figure 12. Heatmap of differentially presented pathways according to the histologic type of cancer predicted by PICRUSt2

Red colors represent higher abundance and blue colors represent lower abundance. Significance was determined by LDA score >2.9 and $p<0.05$.

Discussion

Although increasing studies have profiled the microbiome in respiratory samples from lung cancer patients, little is known about microbiota profile in lung cancer tissue, the association between the microbiome of resected lung cancer tissue and cancer prognosis, and the metabolic function of the lung microbiota. One of the key findings in our study is that alpha diversity was significantly higher in the normal group than in the cancer group and microbial composition differed according to histologic type and genetic mutation of cancer. When we conducted a stratified sub-analysis to address the association between lung microbiome and the prognosis of lung cancer, microbial compositional difference was noted according to postoperative lung cancer stage and the presence of recurrence. Finally, we found several inferred metagenomic functional pathways enriched in different histologic type of cancer from 16S rRNA data.

A previous study showed that alpha diversity was significantly higher in non-malignant than in tumor lung tissues, but no differences were observed in overall composition (beta diversity) between the tumor and non-malignant samples [8]. Another study by Greathouse et al. demonstrated a lower alpha diversity in normal lung as compared to non-tumor adjacent or tumor tissue [6], which is inconsistent with our finding. The present study revealed decreased bacterial diversity in lung cancer tissues compared to adjacent normal lung tissues as well as compositional differences between normal and cancer groups. This suggested that the dysbiosis of lung cancer microbiome and altered microbial composition in lung cancer might be associated with cancer initiation and/or progression.

Few studies have reported microbiome profile in lung cancer tissue. Liu et al. observed that lung cancer patients had higher prevalence of *Firmicutes* (*Streptococcus*) and *Bacteroidetes* (*Prevotella*) compared to emphysema-only patients [7]. Another study by Apopa et al. found that the predominant phyla in the lung formalin fixed paraffin embedded samples were *Actinobacteria*, *Proteobacteria*, and *Bacteroidetes*. They also found that phylum *Cyanobacteria* was consistently observed in AC samples [22]. We have reported that genus *Romboutsia*, *Christensenellaceae R-7 group*, *Novosphingobium*, *Acinetobacter*, *Rhizobium*,

and *Prevotella* were significantly over-represented in cancer group, with some ASVs of them occurring more frequently than predicted by the neutral community model. A previous study reported that genus *Novosphingobium* is present in more severe chronic obstructive pulmonary disease and increases inflammation in a mouse model of smoke exposure [23]. It might also promote carcinogenesis by the mechanism of creating an inflammatory milieu. In a 16S rRNA gene sequencing and transcriptome analysis of bronchial brushing samples, airway *Veillonella*, *Streptococcus*, and *Prevotella* were associated with upregulation of extracellular signal-regulated kinase (ERK) and phosphoinositide 3-kinase (PI3K) signaling pathways in the airway, which regulate cell proliferation, survival, and differentiation [24]. In this study, species *H. influenzae* was enriched in SCC group compared with normal group and we demonstrated the presence of *H. influenzae* from the pure culture of SCC lung tissues. Ochoa et al. found that exposure of the airway to smoke particulates and nontypeable *H. influenzae* promoted lung cancer cell proliferation by release of interleukin-6 (IL-6) and other inflammatory cytokines, which further activated the signal transducer and activator of transcription3 (STAT3) and nuclear factor kB (NF-kB) pathways in airway epithelium [25]. In addition, several studies reported that airway inflammation induced by nontypeable *H. influenzae* provides a tumor microenvironment that favors lung tumor promotion and progression [26-28]. Lung microbiota could lead to carcinogenesis by several mechanisms such as creation of an inflammatory milieu, metabolic effects of dysbiosis and genotoxicity [4, 29].

In this study, we performed a stratified sub-analysis by the postoperative stage and the recurrence of lung cancer to address the association between lung microbiome and the prognosis of lung cancer. Although Kovaleva et al. did not reveal significant difference in alpha diversity between tumors at different stages, they reported a tendency of alpha diversity increase in tumors of later stages [30]. In contrast, several indexes of alpha diversity were steadily declined from normal to more advanced stage in the present study, reflecting a trend toward better prognosis with higher alpha diversity. In addition, a previous pilot study demonstrated that several microbiota in normal lung tissue were associated with recurrence-free survival, but it did not reveal the association between tumor tissue diversity and overall composition and survival [10]. We found that there was a microbial compositional difference

along with the presence of recurrence during the follow-up period, presenting more heterogenous microbial distribution in the cancer with recurrence group. Representatively, genus *Stenotrophomonas* known as a significant pathogen particularly in patients with obstructive lung cancer [31, 32], was identified as the most predominant in lung cancer with recurrence group.

We further investigated inferred metabolic/metagenomic function of lung microbiome from 16S rRNA data of lung tissues in different histologic type of lung cancer. A study by Cheng et al. showed that the pathways of ribosome, pyrimidine and purine metabolism were overrepresented in lung cancer patients using 16S rRNA sequencing of bronchoalveolar lavage samples [33]. In addition, Apopa et al. showed significant metabolic/metagenomic pathways based on Kyoto Encyclopedia of Genes and Genomes (KEGG) pathways from *Cyanobacteria*-specific sequence reads, comparing between the lung cancer subtypes (AC and SCC). The enriched pathways in AC samples included Peroxisome proliferator-activated receptors (PPAR) signaling pathway and D-glutamine and D-glutamate metabolism [22]. In our study, some pathways including TCA cycle and L-glutamate and L-glutamine biosynthesis were predominant in AC group. Emerging evidence demonstrates that certain cancer cells, especially those with deregulated oncogene and tumor suppressor expression, rely heavily on the TCA cycle for energy production and macromolecule synthesis [34]. Lung cancer cells also require glutamine as a nitrogen source to contribute to many anabolic processes in cancer, and as an anaplerotic carbon source that replenishes TCA intermediates [35]. The microbiome of lung cancer might have played a role in these associated pathways.

The present study had several limitations. First, this study is a cross-sectional design which only illustrates the phenomenon and has a difficulty to infer causality. Second, the study had a relatively small number of patients in each group and confounding factors such as other combined lung disease, the use of immunosuppressants and antibiotics that might have affected the microbial communities. In addition, although microbiota composition differs widely according to racial characteristic [36, 37], this study included only a single race, Asian. Therefore, we could not find the microbial compositional difference by race/ethnicity. Moreover, a previous study reported that respiratory microbiome differs significantly between

the three major anatomical regions: oral/nasal, upper and lower respiratory tract [38]. However, because of the insufficient data regarding to the location of resected lung tissues, we were not able to determine whether microbial composition differed according to the location of tumor. Fifth, because we selected paired normal lung tissues from only AC, EGFR+ patients, it is uncertain whether the results of comparison with normal lung tissues from other histologic type of cancer would be same. Additionally, because we had to exclude 47% of samples with a more stringent threshold (100 sequences per sample) for rarefying samples, we opted to use a less stringent threshold (50 sequences per sample). However, we minimized this limitation by performing sub-analysis with rarefying samples to the depth of 25 and 100 sequences. Finally, the lack of a replication dataset may result in unreliability and further studies with validation cohort are needed.

Conclusion

In conclusion, we showed that alpha diversity was significantly higher in the normal group than in the cancer group and microbial composition differed according to the histologic type and genetic mutation in the cancer group. Then, we revealed that there was a microbial compositional difference along with the postoperative lung cancer stage and the presence of recurrence. Finally, we found several inferred metagenomic functional pathways enriched in different histologic type of lung cancer. These findings suggested that the altered microbial composition in lung cancer might be associated with cancer initiation and/or progression.

References

1. WHO report on cancer: setting priorities, investing wisely and providing care for all. Geneva: World Health Organization; 2020.
2. Liu NN, Ma Q, Ge Y, Yi CX, Wei LQ, Tan JC, et al. Microbiome dysbiosis in lung cancer: from composition to therapy. NPJ Precis Oncol 2020;4(1):33.
3. Ramirez-Labrada AG, Isla D, Artal A, Arias M, Rezusta A, Pardo J, et al. The influence of lung microbiota on lung carcinogenesis, immunity, and immunotherapy. Trends Cancer 2020;6(2):86–97.
4. Maddi A, Sabharwal A, Violante T, Manuballa S, Genco R, Patnaik S, et al. The microbiome and lung cancer. J Thorac Dis 2019;11(1):280–91.
5. Jin C, Lagoudas GK, Zhao C, Bullman S, Bhutkar A, Hu B, et al. Commensal microbiota promote lung cancer development via gammadelta T cells. Cell 2019;176(5):998–1013 e16.
6. Greathouse KL, White JR, Vargas AJ, Bliskovsky VV, Beck JA, von Muhlinen N, et al. Interaction between the microbiome and TP53 in human lung cancer. Genome Biol 2018;19(1):123.
7. Liu Y, O'Brien JL, Ajami NJ, et al. Lung tissue microbial profile in lung cancer is distinct from emphysema. Am J Cancer Res 2018;8(9):1775–87.
8. Yu G, Gail MH, Consonni D, Carugno M, Humphrys M, Pesatori AC, et al. Characterizing human lung tissue microbiota and its relationship to epidemiological and clinical features. Genome Biol 2016;17(1):163.
9. Liu HX, Tao LL, Zhang J, Zhu YG, Zheng Y, Liu D, et al. Difference of lower airway microbiome in bilateral protected specimen brush between lung cancer patients with unilateral lobar masses and control subjects. Int J Cancer 2018;142(4):769–78.
10. Peters BA, Hayes RB, Goparaju C, Reid C, Pass HI, Ahn J. The microbiome in lung cancer tissue and recurrence-free survival. Cancer Epidemiol Biomarkers Prev 2019;28(4):731–40.
11. Bolyen E, Rideout JR, Dillon MR, Bokulich NA, Abnet CC, Al-Ghalith GA, et al. Reproducible, interactive, scalable and extensible microbiome data science using QIIME 2. Nat Biotechnol 2019;37(8):852–7.

12. Martin M. Cutadapt removes adapter sequences from high-throughput sequencing reads. EMBnet J 2011;17(1):10–2.

13. Quast C, Pruesse E, Yilmaz P, Gerken J, Schweer T, Yarza P, et al. The SILVA ribosomal RNA gene database project: improved data processing and web-based tools. Nucleic Acids Res 2013;41(Database issue):D590–6.

14. Gotelli NJ, Colwell RK. Estimating species richness. In Biological Diversity: Frontiers in Measurement and Assesment; Oxford University Press: Oxford, UK, 2011;39–54.

15. Magurran AE. Measuring Biological Diversity; John Wiley & Sons: Hoboken, NJ, USA, 2004.

16. Lozupone C, Lladser ME, Knights D, Stombaugh J, Knight R. UniFrac: an effective distance metric for microbial community comparison. ISME J 2011;5(2):169–72.

17. Huang D, Su X, Yuan M, et al. The characterization of lung microbiome in lung cancer patients with different clinicopathology. Am J Cancer Res 2019;9(9):2047–63.

18. Venkataraman A, Bassis CM, Beck JM, Young VB, Curtis JL, Huffnagle GB, et al. Application of a neutral community model to assess structuring of the human lung microbiome. mBio 2015;6(1).

19. Kim HJ, Kim JJ, Myeong NR, Kim T, Kim D, An S, et al. Segregation of age-related skin microbiome characteristics by functionality. Sci Rep 2019;9(1):16748.

20. Xia F, Zhou X, Liu Y, Li Y, Bai X, Zhou X. Composition and predictive functional analysis of bacterial communities inhabiting Chinese Cordyceps insight into conserved core microbiome. BMC Microbiol 2019;19(1):105.

21. Poje G, Redfield RJ. General methods for culturing *Haemophilus influenzae*. In *Haemophilus influenzae* Protocols; Humana Press: Totowa, NJ, USA, 2003.

22. Apopa PL, Alley L, Penney RB, Arnaoutakis K, Steliga MA, Jeffus S, et al. PARP1 is up-regulated in non-small cell lung cancer tissues in the presence of the Cyanobacterial toxin microcystin. Front Microbiol 2018;9:1757.

23. Rutebemberwa A, Stevens MJ, Perez MJ, Smith LP, Sanders L, Cosgrove G, et al. *Novosphingobium* and its potential role in chronic obstructive pulmonary diseases: insights from microbiome studies. PLoS One 2014;9(10):e111150.

24. Goto T. Airway microbiota as a modulator of lung cancer. Int J Mol Sci 2020;21(9).

25. Ochoa CE, Mirabolfathinejad SG, Ruiz VA, Evans SE, Gagea M, Evans CM, et al. Interleukin 6, but not T helper 2 cytokines, promotes lung carcinogenesis. Cancer Prev Res (Phila) 2011;4(1):51–64.

26. King PT, Sharma R. The lung immune response to nontypeable *Haemophilus influenzae* (Lung Immunity to NTHi). J Immunol Res 2015;2015:706376.

27. Moghaddam SJ, Ochoa CE, Sethi S, Dickey BF. Nontypeable *Haemophilus influenzae* in chronic obstructive pulmonary disease and lung cancer. Int J Chron Obstruct Pulmon Dis 2011;6:113–23.

28. Sriram KB, Cox AJ, Sivakumaran P, Singh M, Watts AM, West NP, et al. Non-typeable *Haemophilus Influenzae* detection in the lower airways of patients with lung cancer and chronic obstructive pulmonary disease. Multidiscip Respir Med 2018;13:11.

29. Xu N, Wang L, Li C, Ding C, Li C, Fan W, et al. Microbiota dysbiosis in lung cancer: evidence of association and potential mechanisms. Transl Lung Cancer Res 2020;9(4):1554–68.

30. Kovaleva O, Podlesnaya P, Rashidova M, Samoilova D, Petrenko A, Zborovskaya I, et al. Lung microbiome differentially impacts survival of patients with non-small cell lung cancer depending on tumor stroma phenotype. Biomedicines 2020;8(9).

31. Safdar A, Rolston KV. *Stenotrophomonas maltophilia*: changing spectrum of a serious bacterial pathogen in patients with cancer. Clin Infect Dis 2007;45(12):1602–9.

32. Brooke JS. *Stenotrophomonas maltophilia*: an emerging global opportunistic pathogen. Clin Microbiol Rev 2012;25(1):2–41.

33. Cheng C, Wang Z, Wang J, Ding C, Sun C, Liu P, et al. Characterization of the lung microbiome and exploration of potential bacterial biomarkers for lung cancer. Transl Lung Cancer Res 2020;9(3):693–704.

34. Anderson NM, Mucka P, Kern JG, Feng H. The emerging role and targetability of the TCA cycle in cancer metabolism. Protein Cell 2018;9(2):216–37.

35. Vanhove K, Derveaux E, Graulus GJ, Mesotten L, Thomeer M, Noben JP, et al. Glutamine addiction and therapeutic strategies in lung cancer. Int J Mol Sci 2019;20(2).

36. Carbone C, Piro G, Di Noia V, D'Argento E, Vita E, Ferrara MG, et al. Lung and gut microbiota as potential hidden driver of immunotherapy efficacy in lung cancer. Mediators Inflamm 2019;2019:7652014.

37. Gupta VK, Paul S, Dutta C. Geography, ethnicity or subsistence-specific variations in human microbiome composition and diversity. Front Microbiol 2017;8:1162.

38. Mendez R, Banerjee S, Bhattacharya SK, Banerjee S. Lung inflammation and disease: A perspective on microbial homeostasis and metabolism. IUBMB Life 2019;71(2):152–65.

국문 요약

목적: 폐암은 전 세계적으로 가장 빈번하게 진단되는 암이며 암으로 인한 사망의 주요 원인이다. 최근 많은 연구를 통하여 폐 미생물 군집은 발암 과정과 암세포에 대한 면역 반응의 주요 조절 인자들 중 하나로 알려졌다. 본 연구에서는 폐암과 정상 폐 조직의 미생물 구성을 평가하고, 폐 미생물 군집과 암의 예후와의 연관성을 조사하며 미생물 군집의 기능적인 프로파일을 예측하고자 하였다.

방법: 2018 년 1 월부터 2019 년 12 월까지 서울아산병원에서 폐암 환자로부터 수술적으로 절제한 216 개의 냉동 폐 조직 (암 162 개, 인접한 정상 조직 54 개)이 후향적으로, 무작위로 선정되었다. 이로부터 추출된 gDNA 를 16S rRNA 유전자의 V4-V5 영역을 표적으로 하는 프라이머를 사용하여 증폭시켜 미생물의 다양성과 구성, 대사 기능을 분석하였고, 환자의 의료 기록은 후향적으로 검토하였다.

결과: 폐암 군은 정상 폐 조직 군에 비해 알파 다양성이 유의하게 낮았다. 미생물의 구성은 암의 조직 유형, 유전자 변이에 따라 차이가 있었으며 폐암 군에서 정상 폐 조직 군에 비해 *Romboutsia*, *Christensenellaceae R-7 group*, *Novosphingobium*, *Acinetobacter*, *Rhizobium*, *Prevotella* 속이 증가되어 있었다. 폐 미생물 군집과 폐암의 예후와의 연관성을 조사하기 위해 하위 분석하였을 때 수술 후 폐암의 병기와 재발 유무에 따라 미생물 구성의 차이가 나타났다. 또한, 폐암의 조직 유형에 따른 미생물의 기능적인 프로파일을 분석하였을 때 선암에서는 시트르산 회로, L-글루타메이트 및 L-글루타민 생합성과 관련된 경로가 주로 발견된 반면, 편평상피세포암에서는 퓨린 및 피리미딘 뉴클레오티드 분해, 포름알데히드 동화 등과 관련된 경로가 우세하였다.

결론: 본 연구에서는 폐암의 미생물 군집이 조직 유형, 유전자 변이에 따라 차이가 있으며 병기와 재발 등의 예후 요인에 따라서도 차이가 있음을 확인하였고, 폐암 미생물 군집의 대사 기능을 예측하였다. 이러한 발견은 폐암에서 미생물 구성의 변화가 암 발병 및 진행과 연관이 있을 수 있음을 시사한다.

중심단어: 폐암, 정상 폐 조직, 폐 미생물 군집, 16S rRNA